



Passive guided wave tomography for monitoring corrosion in pipes

Tom Druet, Arnaud Recoquillay, Bastien Chapuis

► To cite this version:

Tom Druet, Arnaud Recoquillay, Bastien Chapuis. Passive guided wave tomography for monitoring corrosion in pipes. 13th European Conference on Non-Destructive Testing (ECNDT 2023), Jul 2023, Lisbon, Portugal. 6 p., 10.58286/28138 . hal-04111455

HAL Id: hal-04111455

<https://hal.science/hal-04111455>

Submitted on 31 May 2023

HAL is a multi-disciplinary open access archive for the deposit and dissemination of scientific research documents, whether they are published or not. The documents may come from teaching and research institutions in France or abroad, or from public or private research centers.

L'archive ouverte pluridisciplinaire **HAL**, est destinée au dépôt et à la diffusion de documents scientifiques de niveau recherche, publiés ou non, émanant des établissements d'enseignement et de recherche français ou étrangers, des laboratoires publics ou privés.



Passive guided wave tomography for monitoring corrosion in pipes

Tom Druet¹, [Arnaud Recoquillay](#)¹ and Bastien Chapuis¹

¹ Université Paris-Saclay, CEA, List, F-91120, Palaiseau, France

arnaud.recoquillay@cea.fr

Abstract

The use of guided waves enables to monitor wide areas of structures with a limited number of sensors and/or a limited acquisition time. In particular, guided wave tomography algorithms give a quantitative image of the residual thickness of the monitored structured, for example a corroded pipe. The idea is to use the dispersion curves to link a change in phase or group velocity to a change in thickness. The method developed at CEA-List includes an auto-calibration phase, eliminating the need of a baseline to work, therefore enabling its use in presence of varying environmental and operational conditions. One drawback of tomography techniques is that they need many sensors compared to more conventional algorithms such as RAPID or Delay and Sum. We propose here a passive version of tomography to limit its intrusiveness by using data obtained by post-processing the ambient elastic noise in the structure. This enables the use of Fiber Bragg Gratings (FBG) on optical fibers as ultrasonic sensors. The use of FBGs drastically reduces the burden of the system, as several gratings can be multiplexed on a single optical fiber. Furthermore, these sensors are suited for many applications because of their resistance to harsh conditions (extreme temperatures, explosive atmosphere, radiations...).

KEYWORDS: guided waves, tomography, passive data, Fiber Bragg Gratings

1. Introduction

Several ultrasonic techniques exist to inspect pipelines, which can be separated in two categories: first, techniques relying on bulk waves are very precise but on rather small areas, needing hence to perform many acquisitions to evaluate the health of a pipe. On the other hand, guided wave techniques are in general relying on the long propagation distance of guided waves, leading to only a few acquisitions but a coarse information on the health state (location of large defects). The technique considered here, namely the guided wave tomography [1][2], is able to reconstruct quantitatively the residual thickness of a pipe wall between two rings of transducers, these two rings being separated by a distance that depends on the configuration of inspection but of the order of a few tens of centimeters. It can hence be used in a NDT context, using two movable rings of

transducers, or in a structural health monitoring context, with fixed rings of transducers, installed permanently to monitor a critical region. Thanks to an auto-calibration method [3], this technique does not need a reference measurement and is hence robust to variations of environmental and operational conditions.

One of the main drawbacks of tomography is it requires a large number of sensors resulting in a potential burden to the structure in terms of added weight or energy consumption. To overcome this issue, we propose a passive technique[1], which consists in the measurement of the ambient noise generated during use of the structure. By doing so, no ultrasonic emission is needed. It is then possible to use ultrasonic sensors unable to emit waves like Bragg gratings on optical fibers. These sensors are suited to harsh environmental conditions (extreme temperature and pressure, radioactivity, insensitive to electromagnetic fields...) and are very small, given that they are just an optical fiber. Furthermore, thanks to multiplexing capabilities, several sensors can be on a single optical fiber, reducing again the intrusivity. We present in more details the different elements of the technique in the next section before giving examples of experimental results.

2. Description of the Technique

2.1 Guided wave tomography

Guided wave tomography algorithms are based on a single mode assumption, which enables the linkage through the dispersion curves of the mode of an information extracted from the signals to the residual thickness of the structure. This information can either be a time of flight, for time of flight tomography methods, linking the group or energy velocity to the residual thickness, or a phase, for diffraction tomography methods, linking the phase velocity to the residual thickness. We consider here iterative diffraction tomography detailed in [3] and initially inspired by [4]. This method is based on the Lippmann-Schwinger equation: for an emitter located at point \mathbf{i} and a receiver located at point \mathbf{j} , the measured scattered field $\varphi^s(\mathbf{x}_j, \mathbf{x}_i)$ at a given frequency ω can be written as

$$\varphi^s(\mathbf{x}_j, \mathbf{x}_i) = \int \mathbf{G}_0(\mathbf{x}_j, \mathbf{x}) \mathbf{O}(\mathbf{x}) \varphi_0(\mathbf{x}, \mathbf{x}_i) d\mathbf{x},$$

Where \mathbf{G}_0 is the Green's function of the Helmholtz equation in the current domain Ω , φ_0 is the unperturbed field and $\mathbf{O}(\mathbf{x}) = \mathbf{k}^2(\mathbf{x}) - \mathbf{k}_0^2$ is the object function, where \mathbf{k} is the wave number and \mathbf{k}_0 is the wave number for the initial thickness. By inverting the Lippmann-Schwinger equation, the object function can be updated iteratively to reconstruct the residual thickness, once again through the dispersion curves linking the wave number to the thickness. Indeed, at step \mathbf{n} , the correction to the object function $\delta \mathbf{O}^n(\mathbf{x})$ can be computed through [1]

$$\delta \mathbf{O}^n(\mathbf{x}) = \int_{-\pi}^{\pi} \int_{-\pi}^{\pi} \frac{\varphi^s(\mathbf{x}_j, \mathbf{x}_i)}{\mathbf{G}_{n-1}(\mathbf{x}_j, \mathbf{x}) \varphi_{n-1}(\mathbf{x}, \mathbf{x}_i)} \mathbf{W}(\theta_i, \theta_j) d\theta_i d\theta_j,$$

where \mathbf{W} is a weighting function coming from a variable change, \mathbf{G}_{n-1} and φ_{n-1} are respectively the Green's function and the solution corresponding to $\mathbf{O}^{n-1}(\mathbf{x}) = \sum_{l=0}^{n-1} \delta \mathbf{O}^l(\mathbf{x})$ and θ_i and θ_j are the angles of the emitter and the receiver respectively.

To compensate for model errors, an autocalibration method is used [3]. The idea is, for all couples, to compute a calibration factor by which the data will be multiplied in order to compensate this error. The calibration factors are computed as

$$c_{ij} = \frac{G_0(x_j, x_i)}{\varphi_0(x_j, x_i)}.$$

As some of the paths of the couples will cross some defect, a confidence ellipse is used to keep only calibration factors corresponding to healthy paths. Paths in the confidence ellipse will use directly their calibration factor. For the remaining paths, the calibration factor is computed as the mean value of the calibration factors inside the confidence ellipse.

2.2 Passive data

Contrary to classic active data acquisitions, as described in the previous section, passive data do not rely on sensors emitting waves. Indeed, it can be proved in the case of diffuse fields [5] that equivalent data to active signals can be recovered. Let φ_i and φ_j be the measured ambient noise by sensors i and j and let $C(x_j, x_i, t; T)$ be their cross-correlation over time window $(0, T)$. It can be shown that

$$\lim_{T \rightarrow +\infty} \frac{\partial C}{\partial t}(x_j, x_i, t; T) \propto F * [\varphi(x_j, x_i, \cdot) - \varphi(x_j, x_i, -\cdot)](t),$$

Where F is linked to the spectral density of the ambient noise. We hence retrieve the impulse response of the system, as if one of the sensors was an emitter, in the frequency domain of the ambient noise.

2.3 Bragg gratings on optical fibers as ultrasonic transducers

Bragg gratings on optical fibers (FBGs) are periodic, or quasi-periodic, local variations in the core of the optical fiber. They can for example be obtained by creating micro-bubbles, inducing a variation in the refractive index. This variation induces the reflexion of light around a center wavelength λ_{Bragg} , with a Gaussian shape for most common FBGs, the value of which depends on the variation step. Strain variations on the fiber, induced by an ultrasonic wave for example, will result in a change in the reflected spectrum. Many techniques for shape or temperature sensing exist nowadays based on FBGs. However, for ultrasonic sensing, a high sensitivity coupled to a high sampling rate are needed, which most methods cannot achieve yet.

The technique used here is the edge filtering (see Figure 1): an interrogating laser source is locked on the edge of the reflection peak, leading to a reflexion of a part of its energy.

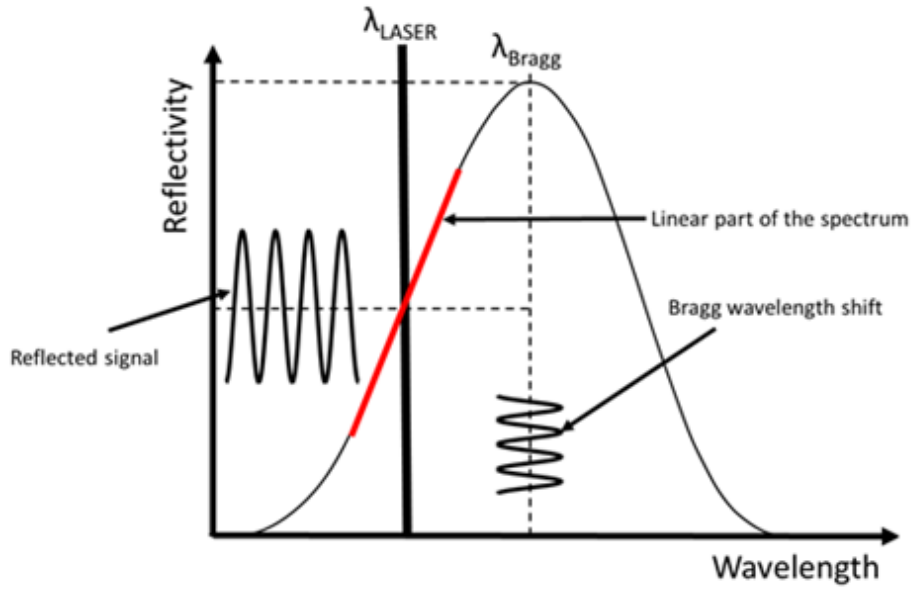


Figure 1: Principle of edge filtering

A photodiode is used to convert the reflected light into a tension, which can be digitized. Due to the ultrasonic waves, the peak will have slight variations around its reference value, which will induce variations in the reflected power. By doing so, high sensitivity can be achieved and the sampling frequency only depends on the one of the digitization, for which nowadays technologies achieve easily several GHz.

3. Results

A stainless steel pipe of outer diameter 125 mm and nominal thickness 2.15 mm was instrumented in two areas. In the first area, two rings of 15 PZT transducers of diameter 7 mm were glued. In the second area, a ring of the same 15 PZT transducers and a ring of 15 FBGs were used. The rings are in both cases 400 mm apart along the axis. Defects were electro-eroded before obtaining a reference image using a 3D profilometer. In the first area (see Figure 2), passive data were acquired by spraying pressurized air inside the pipe. A working frequency of 40 kHz was used.

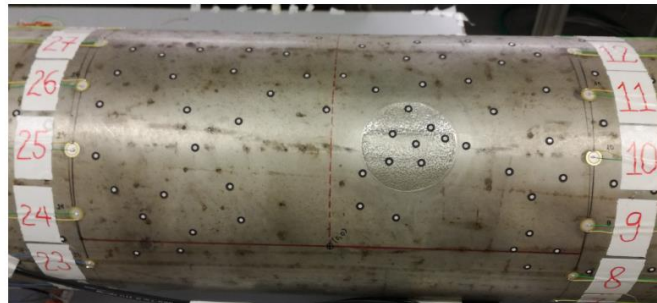


Figure 2: Picture of the instrumented pipe on which passive data were acquired. A defect was electro-eroded.

A reconstructed image using the passive guided wave tomography is shown in Figure 3 using an unrolled view of the pipe, for a 2D representation. The defect is well located.

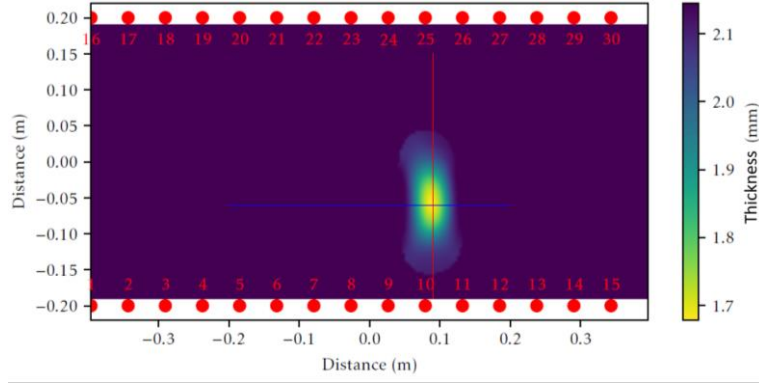


Figure 3: Passive reconstruction. Blue and red lines denote the cut line used in the following picture

More precisely, cut along circumferential and axial lines are plotted in Figure 4. It can be seen that the maximum thickness loss is well retrieved with a precision below the tenth of millimeter. The details of the defect are missing in the reconstruction as low frequency data were used. Indeed, the wavelength of the used mode for this frequency is of 22 mm, and we can see from the plots in Figure 4 that the missing details are smaller, which is coherent with the theory behind diffraction tomography. In particular, the resolution is better along the circumference than along the axis, which is expected: in this configuration, sensors are lacking to obtain data from all directions. Adding sensors along the axis should help improve the reconstruction, but did not seem relevant for the application.

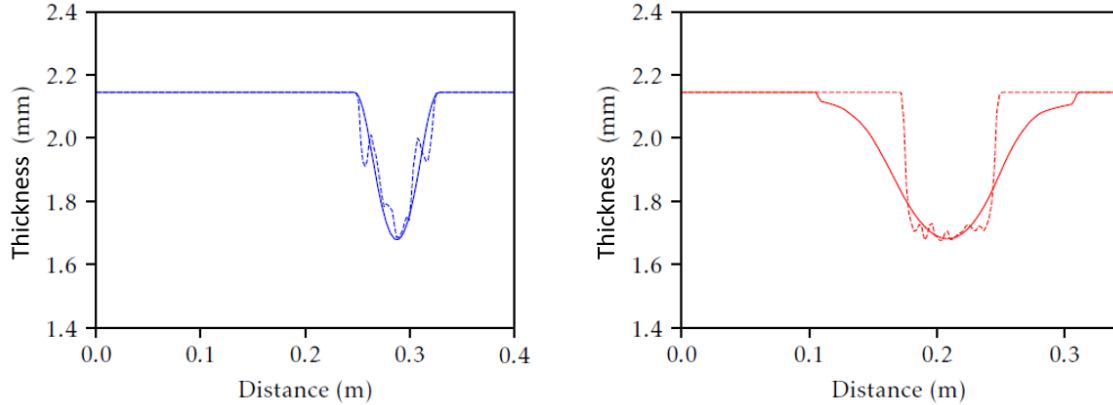


Figure 4: Reconstruction of the defect along the circumference (left) and along the axis (right). The dashed line is the reference.

For the second area, using both PZT and FBGs, active data were used, using PZT as actuators. The results are plotted in Figure 5 and Figure 6. The conclusions of the first case remain valid: the defect is well located and the maximum thickness loss is estimated correctly.

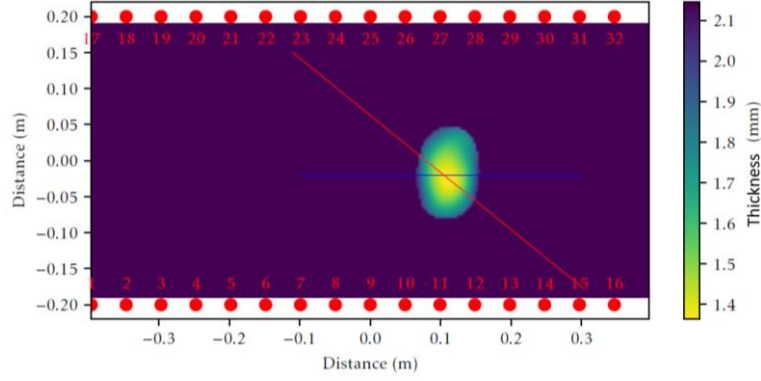


Figure 5: Active reconstruction using a ring of PZT transducers and a ring of FBGs. Blue and red lines denote the cut line used in the following picture

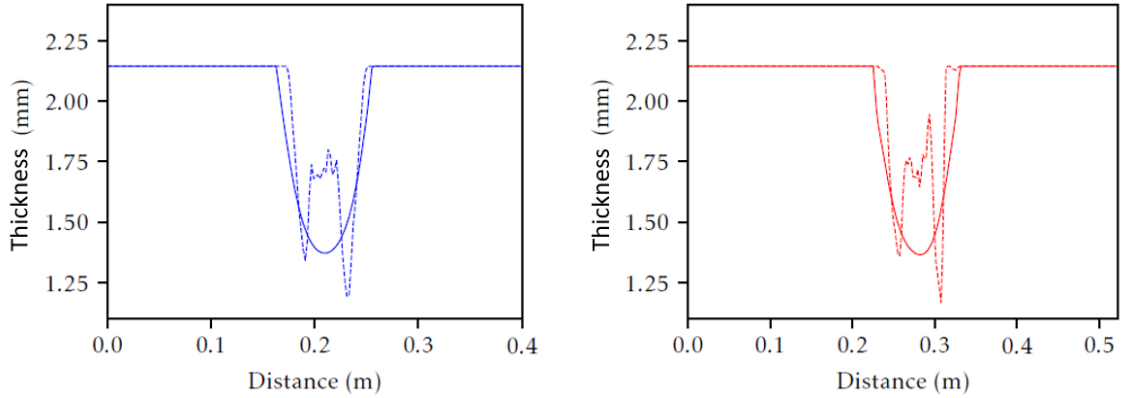


Figure 6: Reconstruction of the defect along the circumference (left) and along the axis (right). The dashed line is the reference.

4. Conclusion and perspectives

We have shown here that passive tomography allows to reconstruct the residual thickness in critical zones of pipelines. More precisely the full method, using ambient noise measurements as input, was validated using classic piezoelectric transducers. FBG sensors were used combined with piezoelectric transducers as actuators in another tomography experiment, showing the possibility to use such sensors. Further tests coupling all these elements, that is using FBGs to measure ambient noise before using guided wave tomography to recover the residual thickness is yet to be performed. Note that FBGs were already used for passive qualitative imaging on plates [6].

References

- [1] Druet, T., Recoquillay, A., Chapuis, B., & Moulin, E. (2019). Passive guided wave tomography for structural health monitoring. *The Journal of the Acoustical Society of America*, 146(4), 2395-2403.
- [2] Hoang, H. T. (2020). Contrôle santé intégré passif par ondes élastiques guidées de tuyauteries pour applications nucléaires et pétrolières.
- [3] Druet, T., Tastet, J. L., Chapuis, B., & Moulin, E. (2019). Autocalibration method for guided wave tomography with undersampled data. *Wave Motion*, 89, 265-283.

- [4] Huthwaite, P., & Simonetti, F. (2013). High-resolution guided wave tomography. *Wave Motion*, 50(5), 979-993.
- [5] Lobkis, O. I., & Weaver, R. L. (2001). On the emergence of the Green's function in the correlations of a diffuse field. *The Journal of the Acoustical Society of America*, 110(6), 3011-3017.
- [6] Recoquillay, A., Druet, T., Nehr, S., Horpin, M., Mesnil, O., Chapuis, B., ... & d'Almeida, O. (2020). Guided wave imaging of composite plates using passive acquisitions by fiber Bragg gratings. *The Journal of the Acoustical Society of America*, 147(5), 3565-3574.